Ab Initio and Nonlocal Density Functional Study of 1,3,5-Trinitro-*s*-triazine (RDX) Conformers

Betsy M. Rice* and Cary F. Chabalowski

U.S. Army Research Laboratory, AMSRL-WM-PC, Aberdeen Proving Ground, Maryland 21005-5066

Received: June 24, 1997; In Final Form: August 28, 1997[⊗]

Geometry optimizations and normal-mode analyses of three conformers of 1,3,5-trinitro-*s*-triazine (RDX) are performed using second-order Moller−Plesset (MP2) and nonlocal density functional theory (DFT) methods. The density functional used in this study is B3LYP. The three conformers of RDX are distinguished mainly by the arrangement of the nitro groups relative to the ring atoms of the RDX molecule. NO_2 groups arranged in either pseudo-equatorial or axial positions are denoted with (E) or (A), respectively. The AAE conformer has C_s symmetry and is the structure in the room-temperature stable crystal (α-RDX). The AAA and EEE conformers have C_{3v} symmetry, a symmetry consistent with vapor and β-solid infrared spectra. The AAE and AAA conformers are studied at the MP2/6-31G*, B3LYP/6-31G*, and B3LYP/6-311+G** levels, and the EEE conformer is studied using the B3LYP density functional and the 6-31G* and 6-311+G** basis sets. The geometric parameters and infrared spectra of the AAA conformer are in good agreement with experimental gas-phase and β-solid data, supporting the hypotheses derived from experiment that the AAA structure is the most probable conformer in vapor-phase and β-solid RDX. The B3LYP/6-311+G** structures and simulated infrared spectra are in closest overall agreement with experimental data. The MP2/6-31G* structures and spectra are in poorest overall agreement with experiment.

I. Introduction

Advances in the development of nonlocal density functional theory (DFT)[1] and in computer architectures have allowed for reliable electronic structure investigations of large polyatomic molecules. We have subjected the well-studied explosive, 1,3,5-trinitro-*s*-triazine, commonly known as RDX, to both DFT and ab initio treatments. The results presented here provide atomic-level information about RDX conformers as well as indicate the suitability of current theoretical treatments to systems such as these. In this work, we will determine the geometries of three conformers of RDX and characterize them through normal-mode analyses using electronic structure methods. Comparisons of structural parameters, vibrational frequencies, and simulated infrared spectra against measured properties are given.

There have been attempts at treating RDX with electronic structure and semiempirical theories;[2−3] however, the highest level of theory used for geometry optimizations reported in these studies is the SCF-MO (Hartree−Fock, HF) level using basis sets ranging from STO-3G to 4-21G.[2,3] These levels of calculations can provide a crude approximation to optimized structures; however, known deficiencies in the theory beg for further theoretical treatments to provide a reliable prediction of the system. An example resulting from the deficiencies in the HF theory is seen in the SCF/4-21G calculations of Coffin et al.,[3] in which SCF geometry optimizations were attempted for four conformers of RDX. The four conformers of RDX differ mainly in the position of the nitro groups relative to the ring atoms. The ring atoms are arranged in the chair conformation. The conformers are labeled according to axial (A) or pseudo-equatorial positioning (E) of the nitro groups about the ring. We will adopt the same nomenclature for the conformers in this work. All nitro groups of the AAA conformer occupy axial positions, and all nitro groups of the EEE conformer occupy pseudo-equatorial positions. Both of these conformers belong to the C_{3v} point group. Two nitro groups occupy axial positions on the AAE conformer and the remaining nitro group is in the pseudo-equatorial position. For the AEE conformer, two nitro groups occupy pseudo-equatorial positions and the remaining nitro- group is axial.[3] The AAE and AEE conformers belong to the C_s point group. Figure 1 illustrates all of these conformers except for the AEE species. For clarity, we have not shown the hydrogen atoms or the oxygen atoms of the nitro groups for the AAA, EEE, and AAE conformers in this figure. Normal-mode analyses for each of the SCF/4-21G optimized structures indicated that only the AAA conformer had all real vibrational frequencies and was, therefore, the only stable species predicted at this level of theory. The remaining conformers, each of which had at least one equatorial nitro group, had imaginary frequencies, indicating they were not stable structures.

Neutron diffraction measurements of solid α-RDX (the form that is stable at room temperature) provided the crystal structure and atomic arrangements of the molecules in the crystal.[4] The molecular geometry of α-RDX is consistent with the AAE conformer. This indicates that either the SCF/4-21G level of theory is not sufficient to correctly describe this conformer or that the crystal field stabilizes the AAE conformer in the α-solid. A second crystalline form of RDX exists (β-RDX) but it is extremely unstable, and no direct experimental structural information is available for this form.[5] Karpowicz and Brill recorded the infrared spectra of both α- and β-RDX, as well as RDX in the vapor phase.[5] The infrared spectra of α- and β-RDX had distinct differences, and the fewer modes in the β-solid suggested a higher molecular symmetry than that of α-RDX. Additionally, the β-solid spectrum had features that were similar to vapor-phase RDX.[5] Karpowicz and Brill concluded that the molecular conformation of the RDX in the β-solid and in the vapor phase has a molecular symmetry of C_{3v} and suggested two possible structures with this symmetry.[5] One structure has the nitro groups occupying all axial positions (AAA), and one has the nitro groups occupying all pseudo-

[⊗] Abstract published in *Advance ACS Abstracts,* November 1, 1997.

S1089-5639(97)02062-8

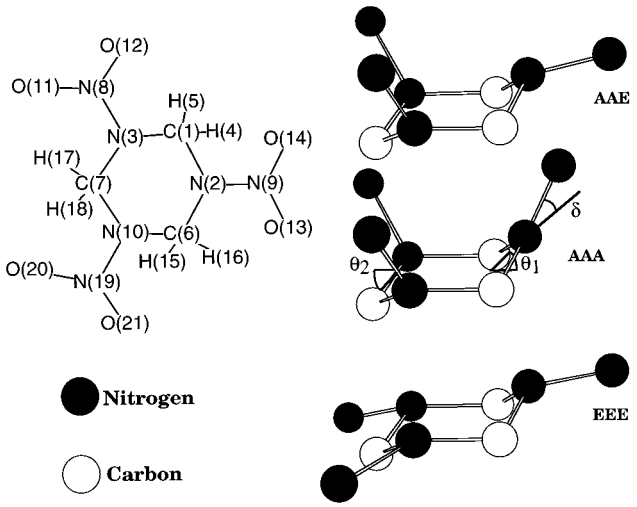

Figure 1. Structures of the AAE, AAA, and EEE conformers of RDX. Atom labels on the two-dimensional projection of the RDX molecule are consistent with the internal coordinates in Tables 1 and 2. The hydrogen and oxygen atoms are not illustrated in the three-dimensional representations for clarity.

equatorial positions (EEE). The measurements did not provide sufficient information to distinguish between the two possibilities. Subsequent electron diffraction experiments indicated that the AAA RDX conformer is consistent with the diffraction patterns, and structural parameters were obtained from fitting models to the experimental data.[6]

We compare ab initio and nonlocal DFT predictions of structural parameters and vibrational frequencies for the AAE, AAA, and EEE conformers of RDX against the experimental information.[4−6] Second-order Moeller−Plesset (MP2)[7] geometry optimizations using the 6-31G* basis set[8−10] are used to locate the AAE and AAA conformers. Nonlocal DFT geometry optimizations using the 6-31G*[8−10] and 6-311+G**[11,12] basis sets and the B3LYP density functional[13−15] are performed for the same conformers and compared against MP2 to determine the magnitude of difference in theoretical treatments. As will be shown, the better agreement of the B3LYP/6-311+G** predictions with experiment strongly suggests that this level is sufficient to accurately determine stable structures for the RDX conformers. Normal-mode analyses are used to characterize each stable point, and infrared vibrational spectra are simulated for comparison with experiment. The spectra are simulated by fitting the predicted infrared intensities to Lorentzian functions with bandwidths arbitrarily set to 8. All calculations are performed using the Gaussian 94 set of quantum chemistry programs.[16] All geometry optimizations meet or exceed the default convergence criteria assigned by Gaussian 94.[16] The DFT calculations use the default grid size given in Gaussian 94.[16]

Results and Discussion

AAE Structural Data. Table 1 lists the geometric parameters of the AAE conformer predicted with various theoretical methods and provides a comparison with parameters obtained from neutron diffraction measurements of α-RDX.[4] The labeling of the atoms in the two-dimensional projection of the RDX molecule in Figure 1 is consistent with the labeling of the internal coordinates in Table 1. The angle θ_1 shown for the AAA conformer in Figure 1 is the angle between the C(1)−N(2)−C(6) plane and the plane containing the C(1)−N(3)−N(10)−C(6) atoms. θ_2 denotes the angle between the planes containing the N(3)−C(7)−N(10) atoms and the C(1)−N(3)−N(10)−C(6) atoms, respectively. The angle δ is the angle between the plane of the C(1)−N(2)−C(6) atoms and the N(2)−N(9) bond. Of the three theoretical treatments, the B3LYP/6-311+G** predictions have the smallest overall deviation from experiment for the bonds and bond angles and the MP2/6-31G* has the largest overall deviation from experiment. The largest differences between theoretical predictions at the three levels presented here and the experimental determinations are in the N−N bond lengths and the C−N−N angles. All of the theoretical predictions overestimate the N−N bond lengths by ∼2.5−4.5%, and the MP2/6-31G* calculations overestimate the N−O bond lengths by 2.1−2.6%. All theoretical methods also overestimate the C(1)−H(4) bond by ∼4%. The B3LYP/6-311+G** predictions of the remaining bonds are in closest agreement with experiment. All of the theoretical methods underestimate the C−N(2)−N bond angles by ∼3.5−6.0%. The MP2/6-31-G* predictions of the remaining C−N−N bonds underestimate the values by 1.5−2.8%, while the B3LYP predictions are within 1% of experiment. The predicted angles θ_1 and θ_2, which are indicative of the deviation of the ring atoms from planarity, are within 3.1 and 2.4% or less, respectively, from the experimental values. The theoretical predictions of δ (which measures the tilt of the N−N bond away from the CNC plane), disagree with experiment by 11.5−15.3° and could be due to crystal field effects. The B3LYP/6-311+G** prediction of δ is in closest agreement with experiment. The overall good agreement in the geometries is remarkable, since the neutron diffraction information was determined from molecules in the crystal state and the theoretical calculations involve a single RDX molecule. The crystal field does not significantly distort the molecule from C_s symmetry.

AAA and EEE Structural Data. The AAA and EEE conformers suggested as possible structures for RDX in the vapor and β-solid phases both have C_{3v} symmetry.[5] Theoretical predictions of geometric parameters for both conformers are given in Table 2 along with the experimental information for vapor-phase RDX. In this table, the individual geometric parameters are given along with the averages of symmetry equivalent parameters. The averages will be compared against the experimental numbers. The theoretical predictions of the bond lengths for both conformers at all levels are within 1% of the experimental result. The agreement of bond angles with experiment, however, is not as good for the C_{3v} conformers as they were for the AAE structure. The largest disagreement between the calculated and experimental values is in the CNC angles. The B3LYP/6-311+G** predictions for AAA and EEE are 115.7° and 117.0°, respectively, which underestimate the experimental value of 123.7° by 8.0−6.7°. The agreement of the MP2/6-31G* AAA prediction of this angle with experiment is even worse (∼10°). It is notable that the theoretical predictions of the CNC angle for these conformers are closer to the experimental value for the AAE conformer (∼114.8°). Shiskov *et al.*[6] note a large change in the CNC angles between the gas-phase and α-solid AAE conformers but attribute the difference to crystal-field effects for the AAE conformer. As mentioned above, this is not supported by the current results where theory (for the isolated AAE molecule) predicts an AAE structure in close agreement with the experimental crystal structure. In addition, the theoretical predictions for the CNC angles are quite similar for all three conformers and agree with the experimental AAE crystal CNC angle to within 2.8° or less. Theoretical predictions of the angles θ_1 are greater than experiment by ∼8° and ∼18° for the AAA and EEE conformers, respectively. These indicate that experiment predicts ring structures closer to planarity than either of the theoretical C_{3v}

TABLE 1: Structural Parameters of the AAE RDX Conformer

Bond (Å)	MP2/6-31G*	B3LYP/6-31G*	B3LYP/6-311+G**	exptl[4]
C(1)−N(2)	1.4700	1.4733	1.4748	1.464
C(1)−N(3)	1.4484	1.4490	1.4488	1.443
C(7)−N(3)	1.4618	1.4621	1.4628	1.468
C(7)−N(10)	1.4618	1.4621	1.4628	1.458
C(6)−N(10)	1.4484	1.4490	1.4488	1.440
C(6)−N(2)	1.4700	1.4733	1.4748	1.450
C(1)−H(4)	1.1001	1.0994	1.0974	1.058
C(1)−H(5)	1.0846	1.0841	1.0827	1.092
C(7)−H(17)	1.0864	1.0851	1.0839	1.085
C(7)−H(18)	1.0936	1.0938	1.0918	1.087
C(6)−H(15)	1.1001	1.0994	1.0974	1.088
C(6)−H(16)	1.0846	1.0841	1.0827	1.075
N(2)−N(9)	1.4105	1.4022	1.4051	1.351
N(3)−N(8)	1.4370	1.4317	1.4335	1.392
N(10)−N(19)	1.4360	1.4317	1.4334	1.398
N(9)−O(13)	1.2360	1.2258	1.2195	1.209
N(9)−O(14)	1.2360	1.2258	1.2195	1.233
N(8)−O(11)	1.2319	1.2202	1.2137	1.203
N(8)−O(12)	1.2324	1.2211	1.2148	1.207
N(19)−O(20)	1.2319	1.2202	1.2137	1.201
N(19)−O(21)	1.2324	1.2211	1.2148	1.205
angle (deg)	**MP2/6-31G***	**B3LYP/6-31G***	**B3LYP/6-311+G****	**exptl[4]**
θ_1	54.14	50.05	50.87	53.31
θ_2	42.74	41.44	41.44	43.73
δ	−27.91	−24.39	−24.08	−12.59
N(2)−C(1)−N(3)	108.84	109.26	109.09	107.8
N(2)−C(1)−H(4)	111.36	110.90	110.64	109.9
N(2)−C(1)−H(5)	109.61	109.38	109.57	110.0
N(3)−C(1)−H(4)	106.90	107.55	107.49	108.0
N(3)−C(1)−H(5)	110.19	109.95	110.30	110.0
H(4)−C(1)−H(5)	109.89	109.78	109.73	111.0
N(3)−C(2)−N(10)	113.38	112.71	112.45	111.7
N(3)−C(2)−H(17)	109.91	109.76	109.99	110.1
N(3)−C(2)−H(18)	106.80	107.21	107.24	106.9
N(10)−C(2)−H(17)	109.91	109.76	109.99	110.7
N(10)−C(2)−H(18)	106.80	107.22	107.24	107.2
H(17)−C(2)−H(18)	109.93	110.09	109.84	110.1
N(10)−C(6)−N(2)	108.84	109.26	109.09	108.4
N(10)−C(6)−H(15)	106.90	107.55	107.49	107.4
N(10)−C(6)−H(16)	110.19	109.95	110.30	111.1
N(2)−C(6)−H(15)	111.36	110.90	110.64	109.6
N(2)−C(6)−H(16)	109.61	109.38	109.57	111.3
H(15)−C(6)−H(16)	109.89	109.78	109.73	108.8
C(6)−N(2)−C(1)	112.76	115.03	114.52	115.1
C(6)−N(2)−N(9)	113.65	115.09	115.42	120.9
C(1)−N(2)−N(9)	113.65	115.09	115.42	119.7
N(2)−N(9)−O(13)	116.52	116.60	116.64	117.2
N(2)−N(9)−O(14)	116.52	116.60	116.64	117.8
O(13)−N(9)−O(14)	126.91	126.78	126.68	125.0
C(1)−N(3)−C(7)	113.88	115.47	115.52	114.6
C(1)−N(3)−N(8)	113.83	116.05	116.43	117.1
C(7)−N(3)−N(8)	114.46	116.51	116.91	116.6
N(3)−N(8)−O(11)	115.78	116.11	116.10	117.2
N(3)−N(8)−O(12)	116.66	116.63	116.65	116.8
O(11)−N(8)−O(12)	127.37	127.11	127.11	125.7
C(7)−N(10)−C(6)	113.88	115.47	115.52	114.8
C(7)−N(10)−N(19)	114.46	116.51	116.91	117.5
C(6)−N(10)−N(19)	113.83	116.05	116.43	115.6
N(10)−N(19)−O(20)	115.78	116.11	116.10	117.3
N(10)−N(19)−O(21)	116.66	116.63	116.65	117.0
O(20)−N(19)−O(21)	127.37	127.11	127.11	125.5

structures, although the AAA values are closer to experiment than the EEE. We have also included the predicted values for γ, which are included in the experimental paper and defined as the sum of the three bond angles involving the ring nitrogen atom. This value reflects the degree to which the ring nitrogen is coplanar with its three attached neighbors. This parameter for both conformers at all levels is in close agreement with experiment.

The geometric parameter ϕ, defined by Shishkov et al.[6] as the torsional angle about the N−N bond, was reported to be 19.1°. The value for the optimized structures calculated at all levels in this study is 0°, indicating a geometry in which the "C...C and O...O lines of the C_2N-NO_2 fragment are coplanar."[6] A geometry optimization of the AAA conformer at the B3LYP/6-31G* level was attempted in which the starting geometry had the angle ϕ set to 19.3°. The value of the angle ϕ in the resulting optimized structure is 0°, and the remaining geometric parameters are equal to those given in Table 2. The discrepancy between theory and experiment could be related to the fitting procedure used in the experimental analysis. In the experimental

TABLE 2: Structural parameters for the AAA and EEE RDX conformers[a]

	AAA			EEE		
	MP2	B3LYP		B3LYP		
	6-31G*	6-31G*	6-311+G**	6-31G*	6-311+G**	exptl[6]
			CN			
C(1)-N(2)	1.4586	1.4603	1.4607	1.4612	1.4612	
C(6)-N(2)	1.4586	1.4601	1.4608	1.4606	1.4612	
C(6)-N(10)	1.4586	1.4604	1.4607	1.4596	1.4604	
C(7)-N(10)	1.4586	1.4599	1.4605	1.4604	1.4605	
C(7)-N(3)	1.4586	1.4606	1.4607	1.4575	1.4593	
C(1)-N(3)	1.4586	1.4606	1.4605	1.4577	1.4598	
⟨CN⟩	1.4586	1.4603	1.4607	1.4595	1.4604	1.464
			NN			
N(2)-N(9)	1.4280	1.4230	1.4237	1.4011	1.4043	
N(10)-N(19)	1.4280	1.4223	1.4236	1.4010	1.4041	
N(3)-N(8)	1.4280	1.4223	1.4229	1.3987	1.4030	
⟨NN⟩	1.4280	1.4225	1.4234	1.4003	1.4038	1.413
			NO			
N(8)-O(11)	1.2331	1.2219	1.2157	1.2254	1.2189	
N(8)-O(12)	1.2331	1.2221	1.2156	1.2255	1.2189	
N(9)-O(13)	1.2331	1.2219	1.2155	1.2251	1.2187	
N(9)-O(14)	1.2331	1.2218	1.2156	1.2252	1.2188	
N(19)-O(20)	1.2331	1.2219	1.2157	1.2252	1.2188	
N(19)-O(21)	1.2331	1.2222	1.2156	1.2252	1.2187	
⟨NO⟩	1.2331	1.2220	1.2156	1.2253	1.2188	1.213
			CH			
C(1)-H(4)	1.0947	1.0947	1.0929	1.1041	1.1022	
C(6)-H(15)	1.0947	1.0947	1.0928	1.1043	1.1023	
C(7)-H(18)	1.0947	1.0948	1.0928	1.1043	1.1022	
C(1)-H(5)	1.0866	1.0854	1.0843	1.0846	1.0830	
C(6)-H(16)	1.0866	1.0854	1.0843	1.0844	1.0828	
C(7)-H(17)	1.0857	1.0856	1.0843	1.0845	1.0829	
⟨CH⟩	1.0905	1.0901	1.0886	1.0944	1.0926	1.089
			NCN			
N(2)-C(6)-N(10)	113.64	112.71	112.47	106.07	105.92	
N(2)-C(1)-N(3)	113.64	112.79	112.43	105.97	105.82	
N(3)-C(7)-N(10)	113.64	112.72	112.46	105.92	105.73	
⟨NCN⟩	113.64	112.74	112.45	105.99	105.82	109.4
			CNC			
C(1)-N(2)-C(6)	114.08	115.50	115.68	117.62	116.95	
C(6)-N(10)-C(7)	114.08	115.67	115.72	117.44	116.90	
C(1)-N(3)-C(7)	114.08	115.62	115.80	117.88	117.12	
⟨CNC⟩	114.08	115.60	115.73	117.65	116.99	123.7
			CNN			
C(1)-N(2)-N(9)	116.08	117.45	117.94	115.13	115.56	
C(1)-N(3)-N(8)	116.07	117.43	118.10	115.89	116.01	
C(6)-N(2)-N(9)	116.08	117.40	117.94	115.09	115.53	
C(6)-N(10)-N(19)	116.08	117.46	117.99	115.31	115.69	
C(7)-N(10)-N(19)	116.08	117.51	118.00	115.31	115.72	
C(7)-N(3)-N(8)	116.08	117.48	118.10	115.93	116.01	
⟨CNN⟩	116.08	117.46	118.01	115.44	115.75	116.3
			ONO			
O(11)-N(8)-O(12)	127.24	127.00	126.97	126.95	126.83	
O(13)-N(9)-O(14)	127.24	127.04	126.98	126.98	126.84	
O(20)-N(19)-O(21)	127.24	127.00	126.99	126.98	126.85	
⟨ONO⟩	127.24	127.01	126.98	126.97	126.84	125.5
			HCH			
H(4)-C(1)-H(5)	109.89	110.09	109.79	109.39	109.56	
H(17)-C(7)-H(18)	109.89	110.02	109.81	109.41	109.59	
H(15)-C(6)-H(16)	109.89	110.09	109.79	109.37	109.55	
⟨HCH⟩	109.89	110.07	109.80	109.39	109.57	105.1
ϕ	−0.03	−0.01	−0.07	−0.01	0.07	19.1
θ_1	42.25	41.75	42.09	51.36	52.45	33.9
θ_2	42.07	40.48	40.65	45.80	47.00	
δ	23.37	19.70	18.41	−21.01	−21.38	19.9
γ	346.24	350.50	351.75	348.54	348.56	356.3

[a] Bond lengths in angstroms, and angles in degrees.

analysis, structural models were assumed, each of which was described by a set of variables that would be parametrized to provide best agreement with the electron diffraction measurements. Three assumptions were made about structural relationships that were held fixed throughout the fitting procedures: The CH_2 moieties have local C_{2v} symmetry, the CNN angles

TABLE 3: Theoretical and Experimental Vibrational Frequencies for RDX Conformers[a,b,c]

	AAE Conformer								AAA conformer							EEE conformer		
	theoretical AAE					α-solid			theoretical AAA					vapor	β-solid	theoretical EEE		
	MP2/6-31G*		B3LYP/6-311+G**			ref 5	ref 17		MP2/6-31G*		B3LYP/6-311+G**			ref 5	ref 5	B3LYP/6-311+G**		
ν	freq	int	freq	int	irr. rep.	IR	IR	Raman	freq	int	freq	int	irr. rep.	IR	IR	freq	int	irr. rep.
1	3277	8	3206	10	A	3074 w	3075 s	3075 m	3265	9	3194	17	A_1	3065 vw	3075 w	3203	2	A_1
2	3277	13	3205	18	A′				3265	11	3192	18	E			3200	23	E
3	3272	13	3199	17	A	3065 w	3066 s	3067 m	3265	11	3192	17	E		3067 w	3199	22	E
4	3155	11	3081	16	A	3001 w	3001 m	3001 s	3144	28	3070	50	A_1		3005 w	2964	117	A_1
5	3083	2	3016	51	A		2948 w	2949 m	3138	0	3064	1	E			2959	6	E
6	3083	41	3015	4	A′				3138	0	3064	1	E			2958	7	E
7	1842	374	1668	117	A	1592 s	1598 vs	1593 w	1836	158	1658	1123	E	1584 vs	1588 s, sh	1637	126	E
8	1837	97	1648	654	A′	1576 s	1573 vs	1570 vs	1836	158	1658	1122	E			1637	126	E
9	1816	276	1623	504	A′	1539 m	1540 vs	1538 w	1828	0	1627	0	A_2		1458 w	1619	0	A_2
10	1547	127	1496	135	A	1533 m	1532 s	1508 vw	1530	89	1482	220	A_1	1444 m	1441 m, b	1522	11	A_1
11	1529	11	1480	15	A′	1458 m	1459 s	1456 w	1508	26	1466	86	E	1420 m	1419 m	1510	19	E
12	1518	116	1468	123	A	1436 m	1434 m	1433 w	1508	27	1464	84	E			1509	19	E
13	1445	124	1420	206	A	1423 m	1423 m	1422 sh	1420	8	1403	59	E	1374 m	1383 w	1431	105	E
14	1420	5	1406	19	A′	1388 m	1389 s	1387 w	1420	8	1402	56	E			1430	109	E
15	1395	1	1374	6	A′		1377 sh	1377 w	1407	0	1384	3	E			1366	0	A_2
16	1382	129	1362	8	A′	1351 m	1352 m	1346 w	1407	0	1381	10	E			1350	48	A_1
17	1376	0	1362	172	A	1311 m	1310 s	1309 s	1373	0	1363	1	A_2			1336	85	E
18	1365	543	1337	530	A	1268 s	1275 vs	1273 s	1371	351	1345	1034	A_1	1319 s	1313 s	1334	91	E
19	1322	1156	1299	468	A′				1316	115	1294	546	E	1268 s	1261 s	1297	205	E
20	1320	219	1296	107	A				1316	115	1292	534	E			1295	267	E
21	1305	79	1270	28	A′	1234 m	1234 m	1232 sh	1309	0	1275	11	A_2	1218 w, b	1218 b	1274	167	E
22	1294	218	1264	339	A	1218 m	1219 m	1214 s	1282	96	1252	208	E			1274	163	E
23	1272	198	1238	112	A′	1181 w			1281	96	1250	202	E			1248	21	E
24	1246	49	1230	87	A	1143 w			1258	7	1242	84	A_1			1245	1	E
25	1195	0	1153	8	A′	1039 s	1040 s	1029 w	1184	0	1141	0	A_2		1142 w	1180	0	A_2
26	1069	107	1036	141	A′	1019 w	1019 m		1032	39	1005	192	E	1014 w, b	1018 w, b	1061	426	E
27	1040	529	1011	588	A	947 m	947 m	943 w	1032	39	1005	209	E			1059	416	E
28	979	677	951	723	A	925 s	926 s	∼920 w	952	180	935	574	A_1		931 m	993	38	A_1
29	967	429	937	922	A	915 s	915 sh		937	184	907	1374	E	910 s	904 s	990	147	E
30	954	689	909	120	A′	883 m	883 m	884 vs	937	184	906	1364	E			989	149	E
31	912	113	896	235	A	853 w	853 w	855 sh	908	1	887	113	A_1	880 m	877 m	910	209	A_1
32	864	477	870	53	A′	844 w	844 w	847 s	856	24	864	3	E	845 w	845 w	888	126	E
33	859	113	855	175	A	782 m	783 s	786 w	856	24	863	1	E			888	125	E
34	803	321	803	292	A		755 m	756 vw	783	116	782	471	A_1	782 m	774 m	819	25	A_1
35	766	29	769	18	A				748	3	754	0	E			763	25	E
36	756	16	761	0	A′				748	3	753	0	E			762	43	A_1
37	740	9	756	21	A	739 m	738 vw	739 vw	727	3	749	6	A_1			761	26	E
38	675	35	676	34	A		670 vw	669 w	668	4	661	33	E			701	3	E
39	657	0	651	4	A′		602 m	605 m	668	4	660	33	E			701	3	E
40	618	67	610	95	A		588 m	589 m	590	9	593	0	A_2			666	0	A_2
41	592	36	588	3	A′				592	9	590	74	E			589	64	E
42	577	19	579	70	A′		486 w	486 w, sh	592	0	590	71	E			588	64	E
43	512	172	463	22	A		461 w	463 m	506	27	458	246	A_1			362	6	E
44	482	77	438	54	A		410 w	414 m	484	5	442	59	A_1			361	6	E
45	434	1	406	84	A				441	1	413	9	E			350	0	A_2
46	432	64	403	6	A′				441	1	409	9	E			331	9	A_1
47	398	0	371	1	A′		345 vw	347 w	388	0	365	3	E			329	111	A_1
48	336	19	325	31	A				388	0	363	3	E			235	149	E
49	293	0	290	0	A′		223 vw	224 vs	292	0	301	0	A_2			232	149	E
50	250	37	229	31	A		208 vw	205 m	232	3	221	96	E			167	26	E
51	217	112	209	15	A′		104	106	232	3	220	94	E			164	31	E
52	137	3	107	0	A			90	132	0	102	58	E			115	28	E
53	86	11	93	10	A′				131	0	100	0	E			114	24	E
54	67	0	74	1	A′				102	0	67	5	A_1			81	0	A_2
55	65	72	63	18	A				36	0	63	8	A_2			62	781	A_1
56	60	111	60	11	A				32	0	37		E			54	46	E
57	37	2	44	2	A′				32	0	31		E			52	44	E

[a] vs = very strong, s = strong, m = medium, b = broad, sh = shoulder. [b] Frequencies and corresponding infrared intensities are in cm^{-1} and $esu^2\ cm^2$, respectively. [c] Symmetry assignments correspond to the B3LYP/6-311+G** results only.

within a molecule are equal, and the NO_2 geometry is planar. The final geometry was obtained by an iterative fitting procedure in which one parameter was optimized at a time while the remaining parameters were held fixed. Initially, all parameters were assigned starting values taken from the literature for similar compounds. After the iterative parameter refinement, a final simultaneous least-squares fit of the parameter set was performed, resulting in the reported values. Such an iterative procedure could be subject to convergence to a local minimum in the parameter space. This is a possible explanation for the difference between the theoretical and experimental value of ϕ.

The information gained by the bond lengths and angles does not provide sufficient information to distinguish between the C_{3v} conformers, nor do the angles θ_1 and θ_2. However, the predicted values of δ for AAA are in almost exact agreement with the experimental value, while the EEE predictions are off by 41°. Therefore, based primarily on δ and less so on θ_1, the

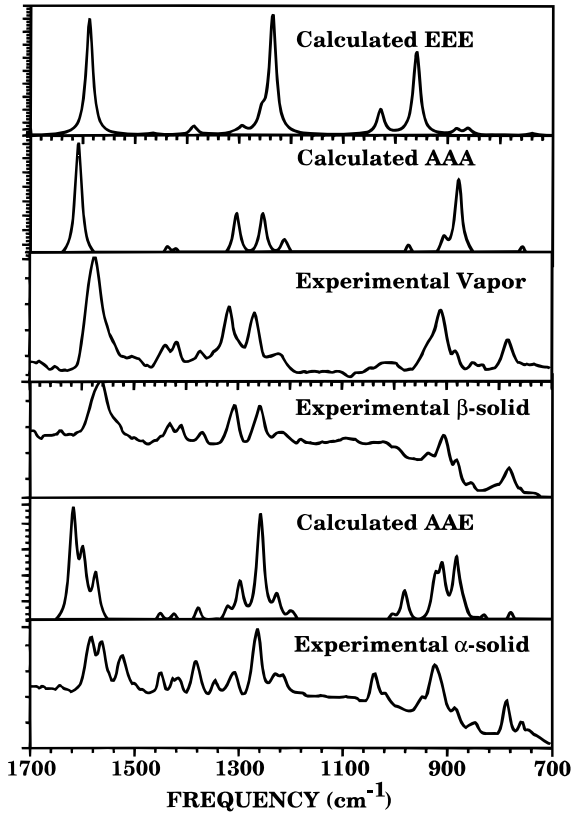

Figure 2. Simulated infrared spectra at the B3LYP/6-311+G** level for the AAA, EEE, and AAE conformers. The vibrational frequencies used to generate these spectra are reduced by 3%. Experimental spectra from ref 5 for α-RDX, *β*-RDX, and vapor-phase RDX are given for comparison.

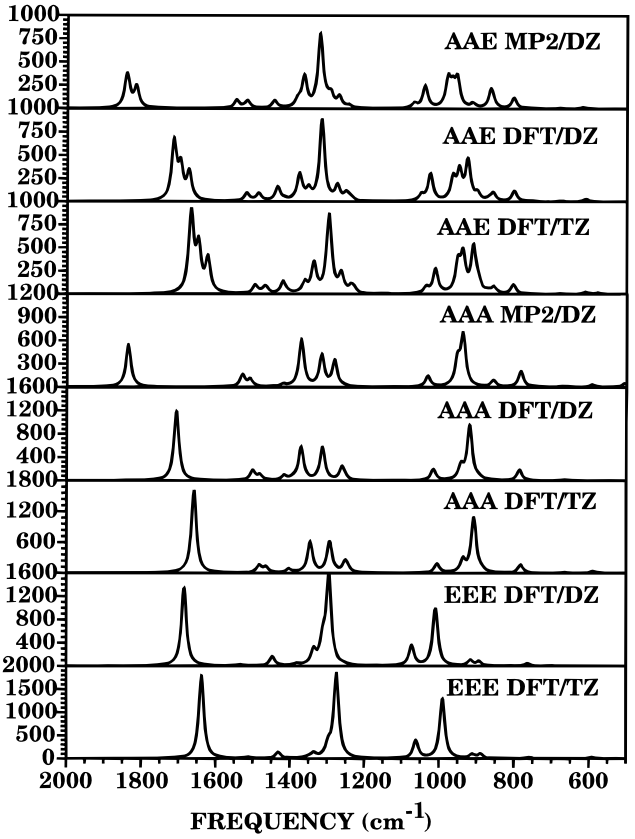

Figure 3. Simulated infrared spectra at the B3LYP level using the 6-31G* and 6-311+G** basis sets for the AAA, EEE, and AAE conformers. MP2/6-31G* spectra are also included. Unscaled vibrational frequencies were used to generate these spectra. DZ denotes the 6-31G* basis set, and TZ denotes the 6-311+G** basis set.

theoretical calculations clearly support the conclusions obtained from the experiment,[6] namely, that the vapor-phase structure of RDX is consistent with the nitro group arrangement in the AAA conformer.

C. Vibrational Spectra. Harmonic vibrational frequencies for the three conformers are determined through normal-mode analyses; each conformer has six zero frequencies and the remaining frequencies are real, in contrast to the SCF/4-21G results.[3] Table 3 provides the calculated harmonic vibrational frequencies at the MP2/6-31G* and B3LYP/6-311+G** levels, corresponding infrared intensities (in esu^2 cm^2), and symmetry assignments for each mode for comparison with the experimental assignments. Assignments identifying the nature of the vibrational modes are given in Supporting Information Table 1S. The symmetry assignments correspond to the B3LYP/6-311+G** results, which appear to give the best reproduction of the experimental spectra, as shown hereafter. It is hoped that these assignments will be of help to experimentalists in interpreting observed spectra.

Simulated spectra based upon B3LYP/6-311+G** infrared intensities and frequencies for the three conformers are compared against experimental infrared spectra in Figure 2. The vibrational frequencies in this figure have been reduced by 3%.

It is clear that the simulated infrared spectrum for the AAA conformer has several features that are similar to the experimental vapor and *β*-solid phase infrared spectra in the mid-infrared region, particularly between 1100 and 1650 cm^{-1}.[5] The theoretical infrared spectrum between 1100 and 1500 cm^{-1} for the EEE conformer shows a band pattern in much poorer agreement with the experimental spectra. These spectra offer strong support for the conclusions of the electron diffraction study that the AAA conformer is the most probable structure of RDX in the vapor phase.[6] These spectra also show that theoretical treatments are useful in differentiating between two possible conformers in the absence of diffraction data. We have also provided a comparison of our simulated AAE infrared spectrum (frequencies reduced by 3%) with the experimental spectrum for the α-solid form in Figure 2. With the exception of the bands around 1040 cm^{-1} in the experimental spectrum, most of the remaining experimental bands can be clearly assigned to a theoretical counterpart. This agreement between theory and experiment seems remarkably good, considering that the experimental spectrum includes effects of the crystal field as well as overtones and combination bands.

Figure 3 provides a comparison of simulated infrared spectra (using unscaled frequencies) for the three conformers at the B3LYP level using the 6-31G* and 6-311+G** basis sets. Figure 3 also includes spectra using MP2/6-31G* results for the AAE and AAA conformers. It is apparent that the features in the B3LYP spectra are relatively insensitive to basis sets. One of the prominent discrepancies between the two basis sets can be seen in all three conformers. This is the shift in the band reported in the 1700-1800 cm^{-1} range at the DZ level to the lower-energy 1600−1700 cm^{-1} range for the TZ basis. A second prominent feature is evident in the AAE spectra and is seen in the relative intensities of the two bands at 1337 and 1362 cm^{-1} from the triple-ζ basis set. These bands can mix since both are of A symmetry, and the 6-311+G** intensity of each band is 530 and 172 esu^2 cm^2, respectively. This ordering agrees with experiment (see Figure 2). The relative locations of these bands appear to be reversed at the double-ζ level. It is apparent that the MP2/6-31G* spectrum for the AAE conformer is substantially different from both B3LYP spectra. The MP2/6-31G* prediction of the spectrum of the AAA conformer also

TABLE 4: Absolute and Relative Energies of RDX Conformers

	MP2/6-31G*			B3LYP/6-31G*			B3LYP/6-311+G**		
	absolute energy (hartrees)	zero-point energy (kcal/mol)	relative[a] energy (kcal/mol)	absolute energy (hartrees)	zero-point energy (kcal/mol)	relative[a] energy (kcal/mol)	absolute energy (hartrees)	zero-point energy (kcal/mol)	relative[a] energy (kcal/mol)
AAE	−895.007 486 8	91.76	0.0	−897.409 356 284	90.06	0.0	−897.679 561 669	89.11	0.0
AAA	−895.007 084 5	91.64	0.13	−897.408 901 632	89.95	0.18	−897.678 331 096	88.98	0.64
EEE				−897.400 693 145	89.59	4.97	−897.671 751 763	88.78	4.57

[a] Zero-point-corrected energies relative to AAE conformer.

has features that differ from the B3LYP predictions, although not as pronounced as for the AAE comparison.

Absolute, relative, and zero-point energies energies of each conformer are given in Table 4. The B3LYP predictions using both 6-31G* and 6-311+G** basis sets indicate that the AAE conformer has the lowest energy of the three conformers, but only by a fraction of a kcal/mol. Similarly, the MP2/6-31G* predictions indicate that the AAE conformer is only slightly lower in energy than the AAA conformer (by 0.13 kcal/mol). The zero-point-corrected B3LYP/ 6-31G* and B3LYP/6-311+G** energies of the AAA conformer are 0.18 and 0.64 kcal/mol, respectively, relative to AAE. Within the level of accuracy for the calculations, the AAE and AAA conformers are identical in their stability. The B3LYP/6-31G* and B3LYP/ 6-311+G** zero-point-corrected energies of the EEE conformer are 4.97 and 4.57 kcal/mol, respectively, relative to AAE. The earlier SCF/4-21G calcalculations had the energy ordering reversed for the AAE and AAA conformers.[3] In that study, the AAA was more stable by 0.6 kcal/mol.[3] Also, the EEE was less stable than AAA by 7.2 kcal/mol.[3] Karpowicz and Brill suggest that the intermolecular forces of neighboring RDX molecules in the α-RDX crystal are responsible for "the energetically unlikely positioning of the NO_2 groups that produces approximately C_s molecular symmetry."[5] The calculations presented here suggest that the positioning of the NO_2 groups in the AAE conformer is not "energetically unlikely."

Conclusions

Three conformers of the large polyatomic explosive RDX have been located and their structures and vibrational spectra characterized with nonlocal density functional theory treatments using double- and triple-ζ quality basis sets. The three conformers have the NO_2 oriented in either axial−axial−equatorial (AAE), axial−axial-axial (AAA), or equatorial−equatorial−equatorial (EEE) arrangements relative to the ring. The AAA structure is consistent with electron diffraction results of vapor-phase RDX,[6] and the AAE conformer is consistent with that of the room-temperature-stable RDX crystal.[4] Additionally, the AAA and AAE conformers are calculated using MP2 theory for comparison with the DFT predictions. Of the three levels of theoretical treatment, the B3LYP/6-311+G** predictions of the geometry of the AAE conformer are in closest overall agreement with experiment, and MP2/6-31G* predictions are in the poorest overall agreement with experiment. The B3LYP/6-311+G** results for the AAE conformer are in agreement with experiment to within 2% for all bond lengths with the exception of a single C−H bond (3.7%) and the N−N bonds (2.5−4.0%). The B3LYP/6-311+G** predictions of bond angles are within 1.6% of experiment with the exception of two C−N−N angles (3.6−4.5%). In general, the B3LYP/ 6-311+G** level produced the closest overall agreement with all available experimental data for structures and spectra.

Structural parameters for the AAA conformer are in closer agreement to experiment[6] than those predicted for the EEE conformer. Additionally, simulated infrared vibrational spectra of the AAA conformer compare well with experimental spectra of vapor-phase and β-solid RDX, while the simulated spectrum of the EEE conformer did not. The differences in predicted geometries and vibrational spectra between the AAA and EEE conformers support the experimental conclusions that RDX in the vapor and β-solid phases have C_{3v} symmetry[5] and have the nitro- groups arranged in the AAA configuration.[6] In addition to providing atomic-level information about a well-studied explosive, the results presented here provide another indication that DFT methods can be applied to large polyatomic molecules with a small computational cost and reliable results for molecular structure, intramolecular force fields, and vibrational spectra.

Acknowledgment. All calculations were performed on the SGI Power Challenge Array at the DOD High Performance Computing Site at the U.S. Army Research Laboratory, Aberdeen Proving Ground, MD.

Supporting Information Available: Harmonic vibrational frequencies and assignment for the RDX conformers (2 pages). Ordering information is available on any current masthead page.

References and Notes

(1) Hohenberg, P.; Kohn, W. *Phys. Rev. B* **1964**, *136*, 864. Kohn, W.; Sham, L. J. *Phys. Rev. A* **1965**, *140*, 113. Zeigler, T. *Chem. Rev. (Washington, D.C.)* **1991**, *91*, 651 and references therein. Labanowski, J., Andzelm, J., Eds. *Density Functional Methods in Chemistry*; Springer: Berlin, 1991. Politzer, P.; Seminario, J. M., Eds. *Theoretical and Computational Chemistry*; Elsevier Scientific: Amsterdam, 1995; Vol. 1.

(2) Habibollahzadeh, D.; Grodzicki, M.; Seminario, J. M.; Politzer, P. *J. Phys. Chem.* **1991**, *95*, 7699.

(3) Coffin, J. M.; Newton, S. Q.; Ewbank, J. D.; Schäfer, L.; Van Alsenoy, C.; Siam, K. *J. Mol. Struct.: THEOCHEM* **1991**, *251*, 219.

(4) Choi, C. S.; Prince, E. *Acta Crystallogr. Sect. B* **1972**, *28*, 57.

(5) Karpowicz, R. J.; Brill, T. B. *J. Phys. Chem.* **1984**, *88*, 348.

(6) Shishkov, I. F.; Vilkov, L. V.; Kolonits, M.; Rozsondai, B. *Struct. Chem.* **1991**, *2*, 57.

(7) Moeller, C.; Plesset, M. S. *Phys. Rev.* **1934**, *46*, 618.

(8) Hehre, W. J.; Ditchfield, R.; Pople, J. A. *J. Chem. Phys.* **1972**, *56*, 2257.

(9) Hariharan, P. C.; Pople, J. A. *Theor. Chim. Acta* **1973**, *28*, 213.

(10) Gordon, M. S. *Chem. Phys. Lett.* **1980**, *76*, 163.

(11) McLean, A. D.; Chandler, G. S. *J. Chem. Phys.* **1980**, *72*, 5639.

(12) Krishnan, R.; Binkley, J. S.; Seeger, R.; Pople, J. A. *J. Chem. Phys.* **1980**, *72*, 650.

(13) Becke, A. D.; *Phys. Rev. A* **1988**, *38*, 3098.

(14) Lee, C.; Yang, W.; Parr, R. G. *Phys. Rev. B* **1988**, *37*, 785.

(15) Meihlich, G.; Savin, A.; Stoll, H.; Preuss, H. *Chem. Phys. Lett.* **1989**, *157*, 200.

(16) Frisch, M. J.; Trucks, G. W.; Schlegel, H. B.; Gill, P. M. W.; Johnson, B. G.; Robb, M. A.; Cheeseman, J. R.; Keith, T.; Petersson, G. A.; Montgomery, J. A.; Raghavachari, K.; Al-Laham, M. A.; Zakrzewski, V. G.; Ortiz, J. V.; Foresman, J. B.; Cioslowski, J.; Stefanov, B. B.; Nanayakkara, A.; Challacombe, M.; Peng, C. Y.; Ayala, P. Y.; Chen, W.; Wong, M. W.; Andres, J. L.; Replogle, E. S.; Gomperts, R.; Martin, R. L.; Fox, D. J.; Binkley, J. S.; Defrees, D. J.; Baker, J.; Stewart, J. P.; Head-Gordon, M.; Gonzalez, C.; Pople, J. A. *Gaussian 94*, Revision B.1; Gaussian, Inc.: Pittsburgh PA, 1995.

(17) Rey-Lafon, M.; Trinquecoste, C.; Cavagnat, R.; Forel, M.-T. *J. Chim. Phys. Chem. Biol.* **1971**, *68*, 1533.